

Detection of a CMB decrement towards a cluster of mJy radiosources

Garret Cotter,¹ Helen J. Buttery,¹ Steve Rawlings,² Steve Croft,² Gary J. Hill,³ Pamela Gay,³ Rhiju Das,^{1*} Niv Drory,⁴ Keith Grainge,¹ William F. Grainger,¹ Michael E. Jones,¹ G. G. Pooley,¹ Richard Saunders¹

¹*Astrophysics, Cavendish Laboratory, Madingley Road, Cambridge CB3 0HE, UK*

²*Astrophysics, Department of Physics, Keble Road, Oxford OX1 3RH, UK*

³*University of Texas at Austin, Astronomy Department, RLM 15.308, TX 78712-1083, USA*

⁴*Universitäts-Sternwarte München, Scheinerstrasse 1, D-81679 München, Germany*

Submitted 2001 March 1; revised 2001 August 22; accepted 2001 September 25

ABSTRACT

We present the results of radio, optical and near-infrared observations of the field of TOC J0233.3+3021, a cluster of milliJansky radiosources from the TexOx Cluster survey. In an observation of this field with the Ryle Telescope (RT) at 15 GHz, we measure a decrement in the cosmic microwave background (CMB) of $-675 \pm 95 \mu\text{Jy}$ on the RT's $\approx 0.65 \text{ k}\lambda$ baseline. Using optical and infrared imaging with the McDonald 2.7-m Smith Reflector, Calar Alto 3.5-m telescope and UKIRT, we identify the host galaxies of five of the radiosources and measure magnitudes of $R \approx 24$, $J \approx 20$, $K \approx 18$.

The CMB decrement is consistent with the Sunyaev-Zel'dovich (SZ) effect of a massive cluster of galaxies, which if modelled as a spherical King profile of core radius $\theta_C = 20''$ has a central temperature decrement of $900 \mu\text{K}$. The magnitudes and colours of the galaxies are consistent with those of old ellipticals at $z \sim 1$. We therefore conclude that TOC J0233.3+3021 is a massive, high redshift cluster. These observations add to the growing evidence for a significant population of massive clusters at high redshift, and demonstrate the effectiveness of combining searches for AGN ‘signposts’ to clusters with the redshift-independence of the SZ effect.

Key words:

cosmic microwave background — cosmology:observations — galaxies:clusters:general — galaxies:active

1 INTRODUCTION

Given a set of cosmological parameters such as Ω_M and Ω_Λ , N -body simulations of the build-up of the mass function of dark matter halos (see e.g. Jenkins et al. 2000) are now sufficiently advanced that there are clear predictions concerning the number of systems of a given mass expected at a given cosmic epoch. At redshifts $z \approx 1$ and beyond, however, only a few members of the population of galaxy clusters are known (e.g. Stanford et al. 1997; Rosati et al. 1999; Chapman et al. 2000; Blanton et al. 2000; Fabian et al. 2001). Here we present the first result of a new technique designed to find distant clusters.

The TexOx Cluster (TOC) survey is an initiative designed to find massive high-redshift clusters. The TOC survey searches

for statistical overdensities of radiosources in the deep, wide area NRAO VLA Sky Survey (NVSS; Condon et al. 1998). Although any search for clusters using AGNs as signposts will find only a small fraction of the total population, the surface density of radiosources is sufficiently low, and the sky coverage of the NVSS sufficiently large, that this technique is very efficient. TOC selects candidates where the radio source overdensity is greater than $5\text{-}\sigma$ in a $7 \times 7 \text{ arcmin}^2$ box. High-resolution VLA followup is used to eliminate the small number of cases where the apparent clustering of sources is spurious, and then optical and infrared imaging are carried out to identify the hosts galaxies of the radio sources and other candidate clusters galaxies.

A full description of the first TOC results will be presented in a forthcoming paper (Croft et al. in preparation; hereafter C2001). In this letter we describe observations of one of the TOC candidates, TOC J0233.3+3021. Our particular motivation in these observations was to exploit the Sunyaev-Zel'dovich (SZ, Sunyaev and

* Present address: Physics Department, Stanford University, CA 94305-4060, USA

Zel'dovich 1972) effect as a means of confirming candidate high-redshift clusters.

In any cluster of galaxies, electrons in the intracluster plasma scatter the CMB photons passing through, distorting the thermal spectrum of the incident CMB and producing a change in brightness temperature given by $\Delta T_{SZ} \propto \int n_e T_e dl$. Here n_e and T_e are the electron number density and Temperature, and dl is an element of line-of-sight element through the cluster. Two consequences of this are:

- Because the CMB imprinting process is a scattering, the same ΔT_{SZ} is produced by a given $\int n_e T_e dl$ whatever the redshift of the cluster.
- The SZ signal from a cluster is less sensitive to mass concentration than either X-ray (emissivity $\propto \int n_e^2 dl$) or optical searches. The integral of ΔT_{SZ} over the projected surface of a cluster is proportional to just the mass–temperature product of the gas.

Observations of the SZ effect in several X-ray selected clusters at $z \gtrsim 0.5$ have now been made using cm-wave interferometers (e.g. Grego et al. 2001, Joy et al. 2001, Grainge et al. 2001). Indeed, the SZ effect is an ideal tool for conducting a survey for clusters, not only because it allows cluster selection to high redshift, but because the selection is limited only by gas mass, almost independently of redshift. Plans have been developed for a new generation of dedicated SZ survey telescopes (e.g. Kneissl et al. 2001, Holder et al. 2000); however, in the absence of an SZ survey, we have undertaken pointed SZ observations of a TOC candidate to confirm that it is a high- z cluster and estimate its mass.

2 OBSERVATIONS AND RESULTS

2.1 Ryle Telescope Observations

The standard configuration of the Ryle Telescope (RT) for SZ observations has been described in detail elsewhere (e.g. Grainge et al. 1996). A nearly-east-west array of five 13-m antennas is used, operating at 15 GHz, giving projected baselines from 13m to 108m (0.65–5.4 k λ). Unresolved sources in the telescope field of view — typically radiogalaxies — contribute equal flux to all baselines of the array, whereas the extended structure of any SZ signal is typically present only on the shortest baseline. We therefore use the long baselines to identify and remove point sources from the field, and use the residual flux on the shortest baseline to measure the SZ flux decrement.

RT observations of the TOC J0233.3+3021 field totalling 280 hours were made during 35 days in the period 1999 January to 1999 June (the declination of the source means that it can only be observed for 8 hours each day). The telescope was in Cb configuration (Grainge et al. 1996), resulting in the aperture-plane coverage shown in Fig. 1. In this configuration the array provides two baselines of maximum projected length 900 λ , three of length 1800 λ , two of 2700 λ and one each of 3600 λ , 4500 λ and 5400 λ . Note that since each day's observation is only eight hours, the baseline tracks in the uv plane are azimuthally truncated. For each day, observations of the target field were interleaved with observations of a phase calibrator about every 20 minutes, and a primary flux calibrator (3C286 or 3C48) was observed at either the start or end of the run.

We analysed the combined 35-day visibility data for evidence of a flux decrement on the shortest baseline. First, we made and CLEANED a naturally-weighted map, using only visibilities from

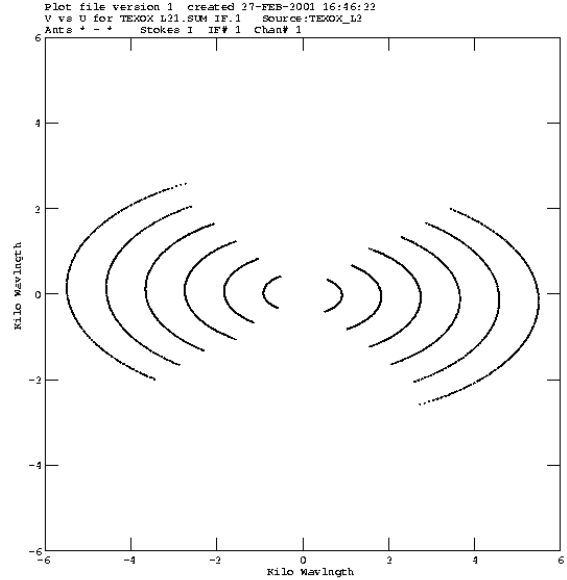


Figure 1. Aperture-plane coverage for the RT observations of the TOC J0233.3+3021 field. Two physical baselines contribute to the shortest baseline in this figure, three to the second-shortest, two to the third shortest, and one to each of the three longest baselines.

projected baselines longer than 1.5 k λ , which is shown in Fig 2, with the NVSS image of the TOC J0233.3+3021 field overlaid. Several of the NVSS sources are readily identifiable on the RT long-baseline map. Next, two of us (HJB and GC) independently investigated the sources present in the RT long-baseline map. We measured the positions of sources in the map using the task MAXFIT in AIPS, then subtracted the brightest source from the visibility data using UVSUB in AIPS. This process was repeated until no sources remained whose peak fluxes were greater than 3.5 times the rms in the map well outside the primary beam. A list of eight sources was agreed upon; all but one of these sources is identifiable on the NVSS map, as shown in Fig 2. Accurate positions and fluxes for these sources were then calculated using the FLUXFITTER algorithm (Grainger et al. 2001). FLUXFITTER takes input estimates of the point-source fluxes and positions, and varies these to minimize χ -squared between the visibility data and model visibilities containing the point sources and noise; it has been demonstrated to produce robust flux and position measurements (Grainger et al. 2001). The resulting source positions and fluxes, calculated using all the data from the projected baselines longer than 1.5 k λ shown in Table 2.1. These sources were then subtracted from all the visibilities. To check that no residual flux from any of the sources was present, source-subtracted maps were made using baselines of length 1.5 k λ and greater (shown in Fig 3), and 2.0 k λ and greater. These maps are both consistent with noise.

Finally, a map was made using source-subtracted visibilities

Table 1. Details of the radio sources in the TOC J0233.3+3021 field, in the following format: Position of source at 15-GHz as subtracted from RT observations; flux at 15 GHz; Position of host galaxy identification (C2001) ; R -, J - and K -band magnitudes (C2001); Label used in Fig. 2.

RT RA (J2000)	RT Dec (J2000)	$S_{15\text{GHz}}$ / mJy	ID RA (J2000)	ID Dec (J2000)	R	J	K	Label
02 33 18.22	30 22 42.91	2.007	02 33 18.1	30 22 40.1	23.75	19.75	18.19	A
02 33 24.97	30 20 09.31	1.906	02 33 25.0	30 20 11.2	23.28	19.74	> 19	B
02 33 11.41	30 25 07.91	1.118						
02 33 31.17	30 22 33.31	1.077	02 33 31.3	30 22 31.2	23.35	20.76	18.58	C
02 33 23.65	30 22 06.41	1.053	02 33 23.7	30 22 00.9	23.10	19.86	18.19	D
02 33 14.23	30 19 46.41	0.497	02 33 14.1	30 19 39.8	24.96	20.82	18.39	E
02 33 38.87	30 21 10.41	0.352						
02 33 22.83	30 19 24.11	0.339						

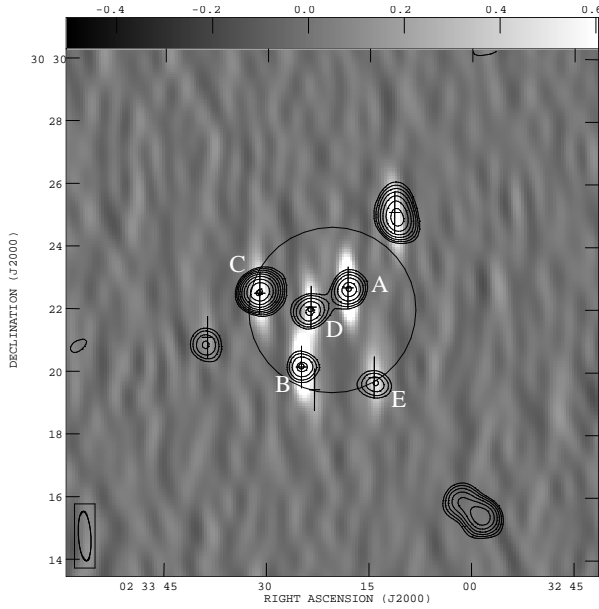


Figure 2. CLEANed 1.5–5.4kλ Ryle Telescope map of the TOC J0233.3+3021 field before source subtraction overlaid with the NVSS 1.4-GHz map of the field (contours). The greyscale runs from -0.5 to $0.6 \text{ mJy beam}^{-1}$, and the contours are $3, 3\sqrt{2}, 6, 6\sqrt{2}, \dots$ multiples of $0.6 \text{ mJy beam}^{-1}$. The large circle shows the FWHM of the RT primary beam, and the ellipse at lower left shows the FWHM of the RT synthesized beam. The five NVSS sources which define the TOC survey overdensity are labelled A–E; the crosses show the positions of the point sources found at 15 GHz. Details of these sources are listed in Table 2.1.

with projected baselines in the range $0.65\text{--}1.0 \text{ k}\lambda$, corresponding to the single shortest physical baseline. This map showed a negative feature centred at $02^{\text{h}} 33^{\text{m}} 20.8^{\text{s}}, 30^{\circ} 21' 58.7''$ (J2000), and with a minimum flux of in the dirty map of $-675 \mu\text{Jy}$. The synthesized beam of this single-baseline map has strong sidelobes, so the rms level on the map even well outside the primary beam is still somewhat affected by the presence of the negative feature at the centre of the map. We therefore made a very large map ($2048 \times 2048 5''$ -square pixels) and measured the map rms in 128-pixel square regions where the map appeared by eye to be unaffected by sidelobes from the central source. The rms levels agreed with the expected noise, due to the telescope system temperature, of $95 \mu\text{Jy}$. The short-baseline map was CLEANed to a flux limit of $-285 \mu\text{Jy}$, and this map is presented in Fig. 4. On inspection of the

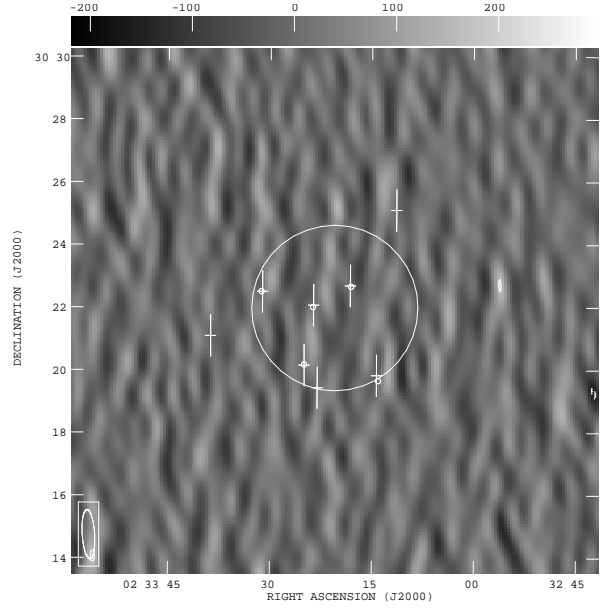


Figure 3. 1.5–5.4kλ Ryle Telescope map of the TOC J0233.3+3021 field after subtraction of the point sources listed in Table 2.1. The greyscale runs from -0.217 to $0.296 \text{ mJy beam}^{-1}$, and contours are plotted at -3 and 3 times $0.050 \text{ mJy beam}^{-1}$, the map rms outside the primary beam. The map is consistent with noise. The primary and synthesized beams are shown as in Fig. 2. The small circles are positions of the five radiogalaxy optical IDs given in Table 1.

azimuthally-averaged visibilities (Fig. 5), the flux on the shortest baseline is $-695 \mu\text{Jy}$, with an rms of $170 \mu\text{Jy}$ (note that since the shortest baseline has an elliptical track in the aperture plane, this rms includes the variation in the amplitude of the SZ signal as a function of uv distance).

2.2 Optical and infra-red observations of the galaxies

We obtained R -band imaging of the TOC J0233.3+3021 field using the Imaging Grism Instrument on the McDonald Observatory 2.7-m Smith Reflector in 1998 October, 1999 October, and 2000 September, and J -band imaging of the field at the Calar Alto 3.5-m telescope in 1999 August. Additionally, we obtained several K -band images of the TOC J0233.3+3021 field with UFTI at UKIRT in 2000 July. Full details, and extensive discussion of other candidate cluster galaxies, will be presented in C2001. Using these im-

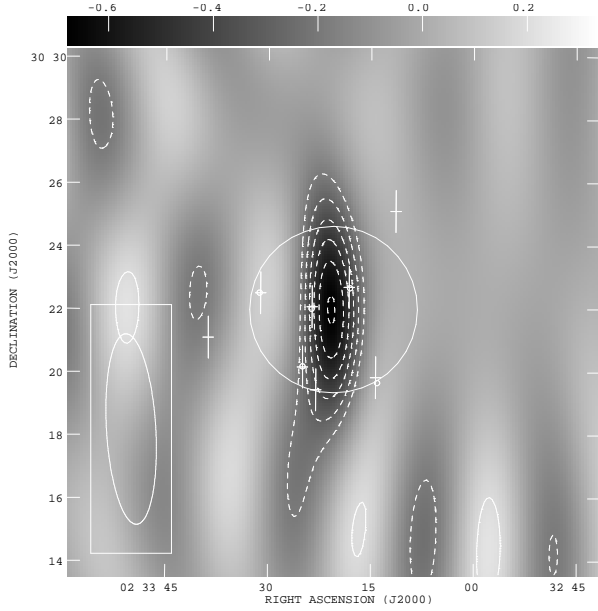


Figure 4. CLEANed 0.65–1.0 k λ Ryle Telescope map of the TOC J0233.3+3021 field after subtraction of the point sources listed in Table 2.1. The greyscale runs from -0.675 to 0.335 mJy beam $^{-1}$. Contours are plotted at $-7, -6, -5, -3, -4, -2$ and 2 times 0.095 mJy beam $^{-1}$, which is consistent with the map rms well outside the primary beam, as described in Section 3.2. Beams and source positions are shown as in previous figures.

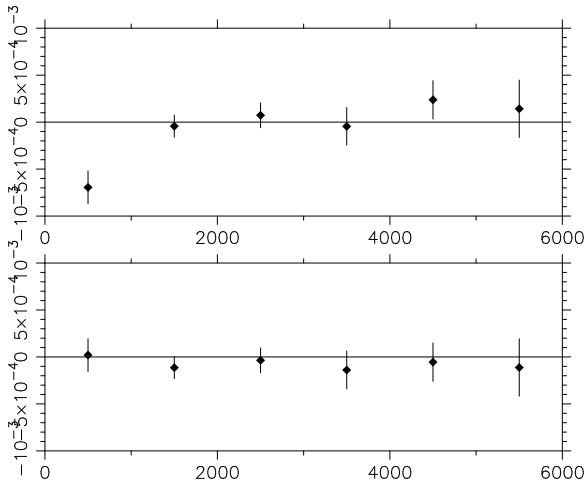


Figure 5. Real (top) and imaginary (bottom) parts of the visibilities, azimuthally averaged about the centre of the decrement after source subtraction. The baseline scale ranges from 0 to 6000 wavelengths, and the flux scale in each plot ranges from -1.0 to 1.0 mJy. The visibilities indicate a single extended negative source at the centre of the field.

ages, in combination with high-resolution VLA imaging (C2001), we have identified the host galaxies of the central five NVSS radio sources shown in Fig. 2. For four of these galaxies, we have obtained $3.5''$ -diameter aperture magnitudes in all filters; for the fifth galaxy, only R and J magnitudes are available. The measured magnitudes of the galaxies are presented in Table 2.1 along with the positions of the host galaxy identifications. The positions were measured from the R -band image, with an astrometric solution using the positions of stars measured in the Cambridge APM survey. The magnitudes of the galaxies are all roughly $K \approx 18$, $J \approx 20$, $R \approx 24$.

In 2000 January, we attempted spectroscopy of the radiogalaxies with ISIS on the WHT. We used a 2-arcsec slit, with sensitivity on the ISIS red arm up to 9340 Å. We took 1800-second spectra of A (at PA=118, the axis of its double structure; see C2001), galaxies B & C (as a pair with PA=113), and galaxies D & E (as a pair with PA=77). Faint red continuum was detected spectroscopically in all the cases expected (i.e. the 4 brightest), but no emission lines were evident.

3 DISCUSSION

3.1 The redshifts of the radiogalaxies

The optical and infrared magnitudes of the radiogalaxies immediately imply that they lie at significant redshift. In particular, given the K -band Hubble diagram for faint radio sources (such as the 7C sample of Willott, Rawlings and Blundell, 2001), the $K \approx 18$ magnitudes of the TOC J0233.3+3021 radiogalaxies suggest that they are L^* galaxies at redshifts of $z \approx 1.0$. We next consider the RJK colours of the radiogalaxies. It is now well-established that faint radiogalaxies at $z \sim 1$ are hosted by Extremely Red Objects (EROs) with colours as red as $R - K \approx 6$. (e.g. Dunlop et al. 1996; Willott, Rawlings and Blundell, 2001). This is consistent with a picture in which faint radio sources at these redshifts are hosted by old elliptical galaxies. Comparing the radiogalaxies with galaxies in the $z = 1.27$ cluster ClG J0848+4453 found by Stanford et al. (1997), we find a close similarity in RJK colour-magnitude diagrams (Fig. 6). If we plot the RJK colours of the radiogalaxies against the track of a redshifted E0 galaxy, we find that they cluster about the $z \approx 1$ region on colour-colour space (Fig. 7). Lastly, the faint red continuum detected in the optical spectra of the radiogalaxies is also consistent with their lying at $z \approx 1$.

These optical and infrared data do not alone demonstrate unequivocally that this overdensity of radiogalaxies is a real cluster. However, the coincidence between the overdensity of sources and the CMB decrement leads us to conclude that we are seeing the SZ effect of a massive cluster, and that most, if not all, the radiogalaxies are cluster members.

3.2 Cluster properties inferred from the SZ effect

From the SZ flux on the shortest spacing, we can now estimate the gas mass of the cluster. We used PROFILE (Grange et al. 2001b) to model the cluster as a spherical King-profile gas distribution, with a gas temperature of 7keV , β -parameter 0.65, and find the best fit value of the central electron density (n_0) to the data for varying core radius θ_C . While the temperature and β parameter are unknown in the absence of deep X-ray imaging, the values we assume are typical of those which have been measured in X-ray selected $z > 0.5$ clusters (see, e.g., Grego et al. 2001 for a summary). For

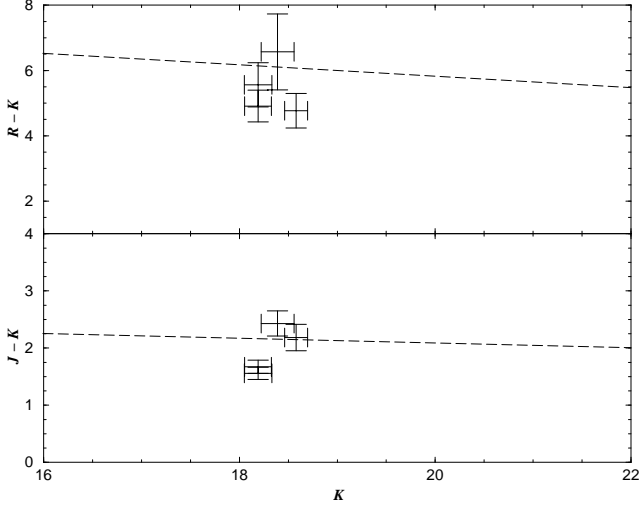


Figure 6. $R - K$ and $J - K$ colour-magnitude plots for the host galaxies of the radio sources; cf Fig. 4 of Stanford et al. (1997). The dashed lines show the red sequence of the galaxies in the $z = 1.27$ cluster identified by Stanford et al. (1997). The similar red colours of the TOC J0233.3+3021 galaxies suggests that they are old elliptical galaxies, with the R and J filters straddling the observed-frame 4000-Å break.

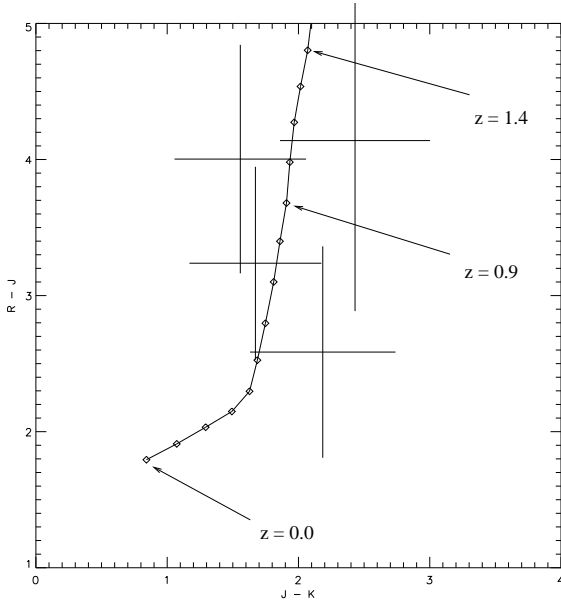


Figure 7. The host galaxies of the radio sources in the RJK colour-colour plane. The radiogalaxies are shown as large crosses, with the size of the cross indicating the photometric errors. The line shows the colours of a non-evolving E0 galaxy as it is redshifted from $z = 0.0$ (lower left), with symbols marking intervals of $\Delta z = 0.1$. The centroid of the radio sources in colour-colour space is at $z \approx 1$.

an $\Omega_M = 0.3, \Omega_\Lambda = 0.7$ cosmology, with $H_0 = 65 \text{ km s}^{-1} \text{ Mpc}^{-1}$, we find that the gas mass within a radius of 1 Mpc is proportional to $\theta_C^{1/2}$. We place the constraint $\theta_C > 20''$ from our measurement that the flux on the second shortest RT baseline is less than $200 \mu\text{Jy}$. This core radius corresponds to a physical distance of 178 kpc and the appropriate best fit model has $n_0 = 10^4 \text{ m}^{-3}$ and a central decrement of $900 \mu\text{K}$. We therefore estimate that the minimum gas mass of the cluster is $5 \times 10^{13} M_\odot$. Assuming that the total mass of the cluster is ten times greater than this, TOC J0233.3+3021 is clearly a massive cluster similar to those identified at $z > 0.5$ in X-ray surveys such as EMSS.

The accurate measurement of the properties of this population of high- z massive clusters is a significant goal in observational cosmology. In this Letter, we have demonstrated that current SZ observations are effective in confirming high- z cluster candidates which have been selected by other means; SZ investigations of other TOC candidates are continuing. The new generation of SZ survey telescopes will not be restricted to the use of ‘signposts’ to high- z clusters, and promise to detect the majority of the distant cluster population.

4 CONCLUSIONS

We have observed the field of TOC J0233.3+3021, a cluster of milliJansky radio sources selected from the NRAO VLA Sky Survey (NVSS), with the Ryle Telescope (RT) at 15 GHz, and in the optical and near-infrared with the McDonald 2.7-m, Calar Alto 3.5-m, and UKIRT. Our conclusions are as follows:

- (i) After subtraction of the baseline-independent fluxes of the radio sources, we find a seven-sigma decrement on the RT shortest baseline of $-695 \mu\text{Jy}$.
- (ii) The radio source host galaxies have magnitudes of $K \approx 18$, $J \approx 20$, $R \approx 24$. From the infrared magnitude-redshift relation for radio sources, the galaxies must lie at $z \gtrsim 0.5$. The similar RJK colours strongly suggest that these galaxies are evolved ellipticals at $z \sim 1$, and the galaxy magnitudes are consistent with the $R - J$ colour-magnitude diagrams of known $z \gtrsim 1$ clusters.
- (iii) We therefore conclude that we have identified a strong SZ decrement with a cluster of galaxies at $z \sim 1$. To produce the SZ decrement, the cluster must have a mass-temperature product similar to that of massive Abell clusters at low redshift; we estimate a minimum gas mass of $5 \times 10^{13} M_\odot$. These observations support the growing evidence for a population of massive clusters at $z \gtrsim 1$.
- (iv) These observations demonstrate the effectiveness of combining searches for AGN ‘signposts’ to clusters with the redshift-independence of the SZ effect. Investigations of this and other high- z cluster candidates selected from NVSS are continuing.

ACKNOWLEDGEMENTS

We thank staff of the the Cavendish Astrophysics group for the operation of the Ryle Telescope, which is funded by PPARC. We thank Joe Tufts for help with the R -band observing, and Chris Willott for help with the ISIS spectroscopy. GC acknowledges a PPARC Postdoctoral Research Fellowship. HJB and SDC acknowledge PPARC PhD studentships. RD acknowledges support from a British Marshall Scholarship. UKIRT is operated by the Joint Astronomy Centre on behalf of PPARC. The WHT is operated on the island of La Palma by the Isaac Newton Group in the Spanish Observatorio del Roque de los Muchachos of the Instituto de

Astrofísica de Canarias. This material is based in part upon work supported by the Texas Advanced Research Program under Grant No. 009658-0710-1999

REFERENCES

- Blanton, E.L., Gregg, M.D., Helfland, D.J., Becker, R.H., White, R.L., 2000, *ApJ*, 531, 118
- Chapman, S.C., McCarthy, P.J., Persson, S.E., 2000, *AJ* 120, 1612
- Condon, J. J., Cotton, W. D., Greisen, E. W., Yin, Q. F., Perley, R. A., Taylor, G. B., Broderick, J. J., 1998, *AJ*, 115, 1693
- Dunlop, J., Peacock, J., Spinrad, H., Dey, A., Jimenez, R., Stern, D., Windhorst, R., 1996, *Nature*, 381, 581
- Fabian, A.C., Crawford, C.S., Ettori, S., Sanders, J.S., 2001, *MNRAS* in press, astro-ph/0101478
- Grainge, K., Jones, M., Pooley, G., Saunders, R., Baker, J., Haynes, T., Edge, A., 1996, *MNRAS*, 278, L17
- Grainge, K., Grainger, W.F., Jones, M.E., Kneissl, R., Pooley, G.G., Saunders, R., 2001a, *MNRAS* submitted, astro-ph/0102496
- Grainge K., Jones M. E., Saunders R., Pooley G. G., Edge A., Kneissl R., 2001b, *MNRAS* submitted
- Grainger, W.F., Das, R., Grainge, K., Jones, M.E., Kneissl, R., Pooley, G.G., Saunders, R., 2001, *MNRAS* submitted, astro-ph/0102489
- Grego, L., et al., 2001, *ApJ* submitted, astro-ph/0012067
- Holder, G.P., Mohr, J.J., Carlstrom, J.E., Evrard, A.E., Leitch, E.M., 2000, *ApJ*, 544, 629
- Jenkins, A., et al, 2001, *MNRAS*, 321, 372
- Joy, M., et al, 2001, *ApJL*, submitted, astro-ph/0012052
- Kneissl, R., Jones, M. E., Saunders, R., Eke, V.R., Lasenby, A.N., Grainge, K., Cotter, G., 2001, *MNRAS* submitted
- Rosati P., Stanford S. A., Eisenhardt P. R., Elston R., Spinrad H., Stern D., Dey A., 1999, *AJ*, 118, 76
- Sunyaev, R. A., Zel'dovich, Ya. B., 1972. *Comm. Astrophys. Sp. Phys.*, 4, 173.
- Stanford, S.A., Elston, R., Eisenhardt, P.R., Spinrad, H., Stern, D., Dey, A., 1997, *AJ*, 114 2232
- Willott, C.J., Rawlings, S., Blundell, K.M., 2001. *MNRAS* in press, astro-ph/0011082